

ALGORITHMS FOR CALCULATING THE 3D CENTER OF ROTATION USING
VICON MOTION CAPTURE SYSTEM AND MATLAB

By
IVAN GRUBISIC

A Thesis Submitted to The Honors College
In Partial Fulfillment of the Bachelor's degree
With Honors in
Engineering Mathematics
THE UNIVERSITY OF ARIZONA

May 2009

Approved by:

A handwritten signature in black ink, appearing to read "David Lomen", is written over a horizontal line.

Dr. David Lomen
Mathematics Department

STATEMENT BY AUTHOR

I hereby grant to the University of Arizona Library the nonexclusive worldwide right to reproduce and distribute my thesis and abstract (herein, the “licensed materials”), in whole or in part, in any and all media of distribution and in any format in existence now or developed in the future. I represent and warrant to the University of Arizona that the licensed materials are my original work, that I am the sole owner of all rights in and to the licensed materials, and that none of the licensed materials infringe or violate the rights of others. I further represent that I have obtained all necessary rights to permit the University of Arizona Library to reproduce and distribute any nonpublic third party software necessary to access, display, run, or print my thesis. I acknowledge that University of Arizona Library may elect not to distribute my thesis in digital format if, in its reasonable judgment, it believes all such rights have not been secured.

SIGNED: _____

A handwritten signature in black ink, consisting of a series of loops and strokes, is written over a horizontal line.

Algorithms for Calculating the 3D Center of Rotation using Vicon Motion Capture System and MATLAB

Ivan Grubisic^{1,2}

May 6, 2009

Abstract

Biomechanical studies are often times interested in understanding what parameters affect how the human body moves in a variety of conditions. Be it after an operation on the lumbar spine, or looking to see how basic physiology of the knee can affect someone's running efficiency. I have attempted to develop an algorithm that will calculate the 3D center of rotation from visual data that has been collected using the Vicon Motion Capture System. The first algorithm, vector addition and subtraction, was disappointing in the application to the lumbar spine, but it does seem to have potential for larger range of motion systems. The 2D projection method showed a lot more promise and seemed to be able to do well within systems where the data points are very close to one another. This success is limited though and would require a further optimization of the parameters and a minimization of the error. Numerical solutions to the problem should also be explored further.

¹University of Arizona, Engineering Mathematics Department

²Orthopedics, Klinikum rechts der Isar der Technischen Universität München

Contents

| | | |
|----------|---|-----------|
| 1 | Introduction | 4 |
| 2 | Materials and Methods | 6 |
| 2.1 | Preparing the lumbar spine | 6 |
| 2.2 | Preparing the knee | 7 |
| 2.3 | Calibrating Vicon | 7 |
| 2.4 | Running a Test Trial | 9 |
| 2.5 | Collecting Vicon Data | 9 |
| 3 | Algorithms | 10 |
| 3.1 | Initial Requirement | 10 |
| 3.2 | Assumptions | 10 |
| 3.3 | Geometric Vector Addition/Subtraction | 11 |
| 3.3.1 | Description of the Method | 11 |
| 3.3.2 | Implementation | 12 |
| 3.3.3 | Applied to the Lumbar Spine | 13 |
| 3.4 | 2D Projection | 14 |
| 3.4.1 | Description of the Method | 14 |
| 3.4.2 | Method Specific Assumptions | 15 |
| 3.4.3 | Implementation | 15 |
| 3.4.4 | Example using a Helix | 16 |
| 3.4.5 | Applied to the Knee | 16 |
| 4 | Potential Improvements | 19 |
| 5 | Conclusion | 20 |
| 6 | Acknowledgements | 21 |
| A | cr-vector.m | 22 |

| | |
|--|----|
| Grubisic | 3 |
| <hr/> | |
| B plane.m | 25 |
| C three-d.m | 27 |
| D two-d.m | 29 |
| E World Congress 2009- Medical Physics and Biomedical Engineering Conference Abstract | 30 |

1 Introduction

Until recently the solution for a dislocation of a vertebral disk between L5 and L4 or L4 and L3 in the lumbar spine has been to fuse L4 to L5 and L3 to L4 using a steel plate. This created more structural support for the patient, but did not provide for much flexibility. Such a procedure also had other drawbacks because it would increase the relative range of motion between L3 and the above vertebrae (L2 and higher). The increased range would cause the cartilage between L2 and L3 to deteriorate faster than it normally would. This would then lead to more operations and possibilities for complications for the patient.

A new implant that is now on the market is provided by ProDisk and is designed in such a way where it directly substitutes for the vertebral disk and is supposed to duplicate the range of motion that is originally found in the lumbar spine. The surgical procedure would still fuse L4 to L5 via a metal plate, but the new implant would be placed between L3 and L4. The increased flexibility of L3-L4 would consequently lead to a decrease in the relative range of motion of L2 and decrease the rate of cartilage deterioration.

It is in the interest of this project to determine if the implant is being placed correctly between the vertebrae. If the center of rotation (CR) of the implant is not placed correctly between the vertebrae, then the natural biomechanics of the lumbar spine would be affected and potentially be more detrimental to the health of the patient than just fusing L3 to L4. At this current time there have been no publications in the literature of a 3D center of rotation calculation done on the lumbar spine. There have been a few instances of researchers solving the 2D problem and in those cases it was noticed that the CR was not a fixed point. Instead it moved within the vertebrae. To

be able to successfully calculate the CR, it is then necessary to make the assumption that between two nearby data points the CR did not move. For that to be true the frequency at which the data is collected should be on the order of at least 25Hz and the speed of the movement should be as slow as possible.

A second study that could use an accurate calculation of the center of rotation was a biomechanical study of the knee. The study was interested in determining if there was a correlation between length of the moment arm and running efficiency. Being able to get accurate, non-invasive measurements of the knee's CR would be a very simple and efficient method with which one could answer the question. The use of MRI data is another non-invasive tool that could be used to measure the CR of the knee, but that requires a secondary step of testing.

In either study, the Vicon Motion Capture System, which uses infrared cameras that detect reflected light, collect the 3D coordinate position of each reflective marker. By taking three point reflective markers and inserting them into vertebrae L1, L2, L3 and L4 it allows each vertebra to be a defined plane. Using the assumption of a rigid body, it is possible to say that any rotation or translation that happens to the marker set is also happening to the vertebra. In the case of the knee, the tibia and femur were described by three reflective markers.

The initial goal of this project was to be able to accurately determine the CR for a variety of systems and to be able to do an intensive error analysis survey of the results. Because of complications during the implementation of the algorithms, and difficulty in acquiring new data, this paper will focus on a few different algorithms that were developed. Each algorithm will be described, assumptions noted and then followed with a discussion of its success, or lack thereof.

2 Materials and Methods

2.1 Preparing the lumbar spine

The lumbar spine that was used in this study was a calf spine that was on the order of 8 weeks old. Once it was received, the musculature and fur were still attached to the spine. It was then the job of the medical student to strip away any superfluous tissues so that the spine was nothing more than the vertebral column. The medical student then continued to screw in a pedicle screw into each vertebra (L1 to L4) at alternating angles from the ventral side. The advantage to doing it in this fashion is that the marker sets that are on adjacent vertebrae will not be obstructing one another's motion. Once the pedicle screws were fixed in the vertebrae, the lumbar spine was taken to have a CT scan conducted of it. The CT scan will then later be used to superimpose the virtual data set onto the actual.

When it was time to test the flexibility of the spine in all directions of interest (flexion, extension and the lateral left and right bends), the lumbar spine had both the top and bottom vertebra (L1 and L4) fixed into a metal box with a polyurethane mixture. When the mixture was dry and both ends of the spine held level, it was possible to attach the marker sets to the pedicle screws. This is the first time that the markers were attached because if they were present earlier it would be possible for them to be scratched and lose some of their reflective material. This would then cause problems with the Vicon's infrared cameras in recognizing where each ball was present.

2.2 Preparing the knee

Much like in the lumbar spine, the joint will be described by two rigid bodies. There will be 3 reflective markers placed on the tibia: one on the center and the other two to the right and left, forming a triangle. The same organization will be used on the femur as well. Unlike in the case of the lumbar spine, there will be no exact data for the center of rotation, and therefore there will be one marker placed on both the left and right sides of the knee. These markers will be placed centrally along the sides of the knee so as to provide a reference frame of where the center of rotation should land, i.e. directly between those points.

2.3 Calibrating Vicon

Vicon consists of six infrared cameras that can be set up on stands and is accurate to 0.5mm. The accuracy was determined by doing a static test, with the same marker sets that would be used in the study, measuring the virtual distance between the points and then comparing them with the actual distance. It is important that each point is recognized successfully by at least two of the cameras. Otherwise it is not possible to get a 3D depiction of where the point is in space. The accuracy of the system also increases when each point is recognized by more than two cameras. Therefore the goal is to set up the stands in such a way that each camera will see every point for the duration of each trial. To do this effectively it is suggested that the spine with the attached marker sets is placed into the testing area, and it is monitored on the computer screen if the points are recognized. The ideal situation is when each of the points is a colored circle on the screen, and is as small as possible. That ensures that the resolution is at a maximum and allows for the smallest type of error. It is also very important that

there are minimal artifacts being recognized by the cameras and that no camera can see another camera in its view. Since the room is large enough to disperse the cameras in a full circle around the test area, this setup will provide for the best visualization of the markers, and therefore minimize the error.

Once the cameras have been set up in such a way that each point will be recognized by at least two cameras, it is possible to calibrate the testing space. After removing the spine from the testing area, the calibration consists of two different steps: the static and dynamic calibrations. Once the necessary cameras have been selected in the Vicon program it asks to first conduct the static calibration. The static calibration requires that a wand with four marker points on it is placed in the testing space. It is important to make sure that this triangle is placed on the base of the testing area because any movement of a marker under this plane will not be calculated into the final data set. Once the static calibration has been completed it is time to do the dynamic. The dynamic calibration consists of using a wand that has three marker points on it of a designated diameter and a specified spacing. The type of wand used needs to also be specified during the first screen of the calibration process. The movement of the wand needs to also encompass the entire testing area and it is also advised that it mimic the expected motion of the marker sets during the trial.

After the calibration a residue value will be associated with each camera that was selected and there will be a static reproducibility value given. The residues should all be as small as possible, but no larger than 0.50. Since the testing area in this study was so small, it should not be an issue to configure the cameras in such a way where it is possible to attain such a small residue. The static reproducibility should also be on the order of 1. Any serious deviation from that would require a recalibration. Once

the cameras have been successfully calibrated it is important that their position is not even slightly altered. If for some reason one of the cameras is affected, then the entire calibration process needs to be done a second time.

2.4 Running a Test Trial

It is advised that the Vicon system be allowed to collect data points for about 10 to 15 seconds before the motion begins because the software occasionally has trouble recognizing all of the points in the first few seconds. The frequency at which the data is collected is initially set at 200Hz, and it can be manually adjusted. For the purposes of this experiment though it was left at 200Hz. The data was then thinned out later in the MATLAB code.

2.5 Collecting Vicon Data

After running a test trial it is possible to see an animation of the movement where each of the marker points is visualized. Vicon does not have the capability of identifying the points itself, but it can track them automatically after they have been identified. To do this it is necessary to write a text file that is imported at the beginning of the trial to be able to label the points. The text file can also be written in such a way where each marker set of three points is grouped together as a single body. An example of a text file can be found in Appendix A, Script 1. This will draw green lines between each of the points and makes it easier to notice if a point goes missing or is relabeled onto another point during the trial. Such errors are easy to correct though through the "Edit" menu in the program.

Once each of the points has been labeled correctly, it is possible to pipeline the data into a CSV file which is readable by Excel. It is important to realize that there is no real order to how the points are imported into the CSV file and therefore it is necessary to either be able to read the headers when the data is later imported into MATLAB or to simply pay attention in Excel to which column refers to which marker point. The data will be broken apart by labeled marker point with the x,y,z coordinates of each.

3 Algorithms

3.1 Initial Requirement

It has been hypothesized that the CR is not a fixed point within the lumbar spine. This stipulation requires that an iterative method be used. The iterative method is not necessarily a numerical solution though. It means that the data points are broken down into subgroups and the CR is solved for from each subgroup. By being able to solve for the CR in n subgroups of the data, it will create a movie of how the CR moves in the system. This is of course not necessary for the knee or other joints in the body that are ball and socket joints, but this methodology will not affect the results in those simulations. The reason for it is because the CR will remain stationary or at most, vary because of noise caused by Vicon.

3.2 Assumptions

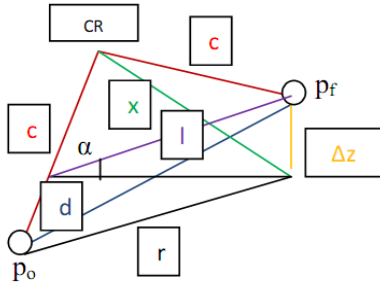
The primary and most important assumption is that no translational motion occurs during any of the subgroups. In the case that there is translational motion, it is below

the precision threshold of the VICON cameras and therefore will be considered to be noise. Since VICON collects data at 200Hz, and the motion of the lumbar spine is at 50mm/s each of the subgroups will contain data that represents only rotational motion.

3.3 Geometric Vector Addition/Subtraction

3.3.1 Description of the Method

This model takes advantage of simple vector addition and subtraction routines. The three markers on the rotating body will be used to define the body as a plane. Solving then for the dihedral angle, α , between the planes initial and final states with respect to the plane $z = 0$ allows us to create a geometric picture of the motion. Figure 1 shows a color labeled diagram of what that geometry looks like from the perspective of one of the markers on the three marker set.



$$r = \sqrt{(x_1 - x_2)^2 + (y_1 - y_2)^2}$$

$$d = \sqrt{(x_1 - x_2)^2 + (y_1 - y_2)^2 + (z_1 - z_2)^2}$$

$$\Delta z = z_2 - z_1$$

$$p_o = (x_1, y_1, z_1)$$

$$p_f = (x_2, y_2, z_2)$$

Figure 1: A geometric representation of the motion of a rigid body with respect to its initial position. The equations on the right describe the values that can be solved for initially. p_o and p_f refer to the initial and final positions, while CR is the center of rotation and c is the radius of curvature.

The key for any vector arithmetic will be decomposing the vectors to their angular and position components. By looking at the system in terms of spherical coordi-

nates, there is the need for two different angles. The first one is ϕ , $\angle p_0 CR p_f$, and ζ , $\angle p_f(x_2, y_2, z_1) CR p_f(x_2, y_2, z_2)$, is the second one. This can be visualized in Figure 1. By applying rules of geometry and using the Sine Law, it is possible to use the given information to solve for the necessary angles. Applying these components, along with the radius of curvature, c , provides us with the necessary array of equations needed to solve for the CR.

$$CR_x = p_{0_x} \pm c \cos\left(\frac{\phi}{2}\right) \quad (1)$$

$$CR_y = p_{0_y} \pm c \sin\left(\frac{\phi}{2}\right) \quad (2)$$

$$CR_z = p_{0_z} \pm c \sin\left(\frac{\zeta}{2}\right) \quad (3)$$

Equations 1 – 3 have a \pm component because it is conceivable that the motion of bending a spine or flexing a knee, would cause the marker points to move from being either positioned positive or negative to the CR. This difference needs to be accounted for in the script, otherwise the calculation of the CR will be limited to only half of the total range of motion.

3.3.2 Implementation

The implementation of this method required the use of two different MATLAB scripts that were written by me. The data is uploaded by `cr-vector.m`, Appendix A, where it is then organized in terms of rigid bodies. This means that each of the three markers that define a single rigid body will be placed into the same matrix. A second function called `plane.m`, Appendix B, is used to define a plane for each step of the iteration. Once all of the angles are decomposed, then the geometry that was mentioned in the

description of the method, would be solved for each step.

3.3.3 Applied to the Lumbar Spine

Applying this method to the lumbar spine was not as successful as it was initially hoped. Figure 3.3.3 shows how the CR moves through 3D space in red and the relative motion of one of the marker points from the set of three in green for L3. Upon initial observation it seems that the CR is moving around in the vertebrae as it would be expected. Since the movement was a lateral bending that went to the left and then back to the right, if the CR was to exhibit any movement, it would be expected to have a symmetrical curve, which is exactly what we see. However, upon closer inspection of the axis, it is clear that the CR never travels further than approximately 25mm away from the reflective marker. Since the pedicle screw that was used to attach the marker sets to the lumbar spine was 180mm long, that is the minimum expected distance away from the marker that we would expect.

Since the reflective marker that was used to calculate for the CR itself did not move very far itself, the relative angle measures between steps were probably very small. Considering that most of the geometric calculations dealt with taking the sine of small angle measures at several steps of the procedure, would probably lead to large errors because $\sin(x)$ for small x is approximately x . Not only is this a potential for error, but it is also not 100 percent clear exactly what angle the dihedral angle α refers to. I have reason to believe that it could be a composition of multiple angle measures because the set of three reflective markers was not necessarily perfectly parallel to the ground when the lumbar spine was perfectly upright. These types of uncertainties do not allow this method to be looked at very seriously. It shows the potential of being able to map the

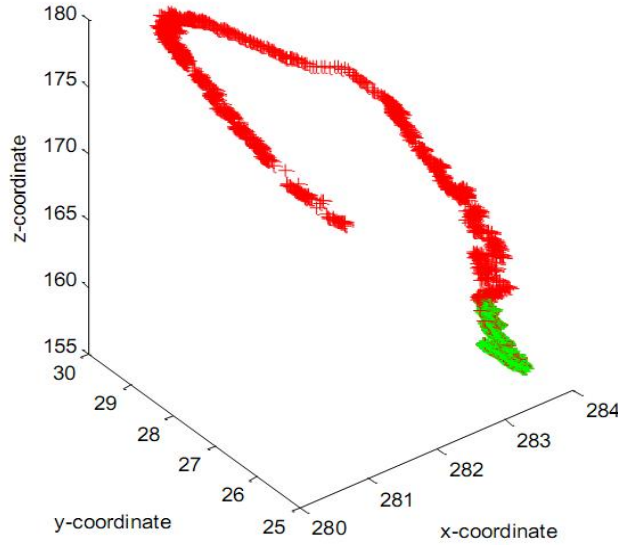


Figure 2: A mapping of the CR, red, as it moves through space for L3 with respect to the reflective marker used for the calculation of the CR, green.

position of the CR, but at the current state, there are still too many bugs either in the script, the precision of MATLAB or simply the accuracy of the Vicon data.

3.4 2D Projection

3.4.1 Description of the Method

Solving for the CR of each subgroup in the three dimensional space will be done by projecting into the 2D space. Which 2D space to project the data points onto will be done by determining which coordinate changed the least in that subgroup by using the *gradient* function in MATLAB. Each subgroup of points will also be described by a

plane so it is possible to solve for the remaining coordinate.

3.4.2 Method Specific Assumptions

A subsequent assumption which follows is that the data points can all be explained by a single plane. This is what allows us to project the data onto the 2D space, solve for the center of rotation, and then using the equation of the plane recursively solve for the third coordinate.

3.4.3 Implementation

The algorithm will be implemented using MATLAB and will have the following steps.

1. Import data set from VICON into MATLAB
2. Define the size of the subgroup and divide the dataset into n groups
3. For each subgroup, determine along which axis there is the least movement using the *gradient* function
4. Determine the equation of the plane for each subgroup
5. Solve for the tangent and normal vectors to the curve
6. Using the backslash operator, solve for the intersection point (i.e. the CR), of the normal vectors
7. Plug in the CR value into the equation of the plane to solve for third coordinate

Using these steps creates a model that is more robust than one that relies on the vector addition and subtraction because the proximity of the points causes the problem

to become poorly conditioned very quickly. This algorithm is implemented by two MATLAB files: `three-d.m` and `two-d.m` which are both found in Appendix C and D respectively.

3.4.4 Example using a Helix

Figure 3(a) shows a very simplified case where the rotation and translation of the points are moving along the z-axis. The data was simulated by manually creating a helix in MATLAB. After applying the above mentioned algorithm, with the exception of a few outliers, the results were very consistent. Taking the outliers into account reports a RMSD of 2.1. When removing the outliers in Figure 3(b), the RMSD decreases to 0.27 which is below the precision of the VICON system. The units were dimensionless in this case, but it could be compared to the millimeter scale that is used by VICON. This means that the the algorithm does not contribute much to the total error of the system. What it is that contributes to the outliers though is not known. Up until now it has not been possible to determine any pattern which could explain the outliers.

It is appropriate to get rid of the outliers because it is reasonable to assume that the movement of the CR through space should be a smooth curve if the data is also a smooth curve. There should not be any drastic jumps.

3.4.5 Applied to the Knee

The application of this method to the bending of the knee has shown some promising results. Figure 3.4.5 shows that there is a clustering of the calculated CR between the two green sets of data points that represent the left and right hand sides of the knee. This was done by looking at every 5th point of the data that was collected at

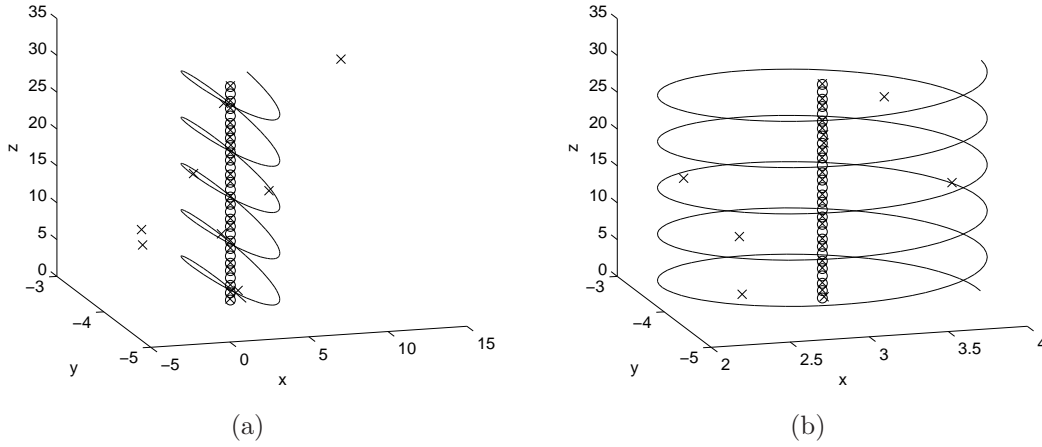


Figure 3: Using MATLAB to solve for the center of rotation of a helix. (a) The plot with all of the calculated values. The actual center of rotation is marked by a 'o' where the calculated is a 'x'. (b) The plot with the three main outliers excluded. The same symbols were used as in part (a).

200Hz. Unlike the vector addition and subtraction method that was described before, it is in the best interest of this algorithm for to have the points as close as possible to one another. Since the *gradient* function is being used in two-d.m, and no additional interpolating function (i.e. *spline*) is being implemented, it is better when the points are very closely spaced.

The only issue with the results as they are right now is that the calculated value of the CR still has a very large range. It is also very dependent on which of the markers from the knee set up described in section 2.2 is used to do the calculation. This indicates that the model is not very robust and still have plenty of room for improvement. When it is known approximately where the CR should lie though, given the results from the helix, I believe that the calculated values that land in that region are going to be accurate. The only way to know for sure though is to compare the results to MRI data and only then will it be possible to know for sure.

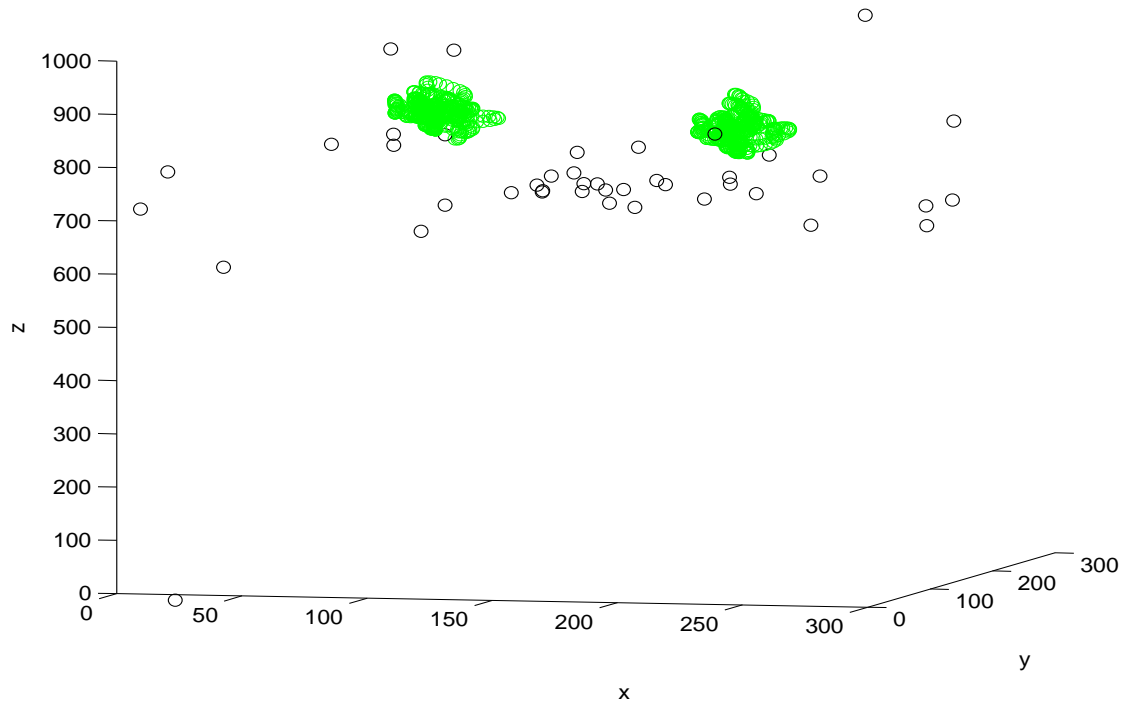


Figure 4: The calculated center of rotation is labeled with a black 'o' and the right and left hand sides of the knee are labeled by a green 'o'.

4 Potential Improvements

In this section we will focus primarily on the second algorithm, the 2D projection, because of the success that it has shown up until this point. An optimization scheme should be used to minimize the error and variability of this method. In its current form, the interval of points that describes the n subgroups has been arbitrarily picked. Figure 3.4.5 used every 5th point, but an intensive error analysis would need to be conducted before we could definitely say that it is an optimum spacing. Another relatively arbitrary part of the code exists in the two-d.m script. The intersection point between two normal vectors is defined arbitrarily as the intersection between the vectors that are at 40 and 80 percent of the total spacing of a given subgroup. Even though for a perfect arc all of the normal vectors will intersect at a single point, i.e. the CR, the Vicon data has a certain element of noise. This noise does not create a perfect arc and therefore depending on which normal vectors are chosen, different centers of rotation can be determined.

One method that could be used to determine the optimum conditions would be to use a large sampling. This means using a random number generator to randomly pick the number of points assigned to each subgroup, and to then run 1,000 to 10,000 runs to see how much the accuracy of the algorithm depends on the subgroup spacing. For each randomly sized subgroup spacing though, it would be of interest to run another 1,000 to 10,000 calculations to see what the actual CR is. It would be reasonable to conclude that the point through which the most normal vectors are passing is the true CR and any variation from that point comes from the noise in the system. The main issue with this sort of method though is that it could be computationally very expensive. A numerical solution for the intersection point may also be more appropriate.

Another way that may be less time intensive is to run a refinement on the data. This could be done using a *spline* function, but since spline functions will fit all the points with a smooth curve, and there is the possibility for the noise in the system to become more apparent. A more effective way would be to interpolate the data points in each subgroup with a parametric set of equations: $x = \cos(t)$, $y = \sin(t)$. This smooth curve would minimize the the variability of the normal vectors and would hopefully make it more robust.

5 Conclusion

In this paper we discussed two different algorithms that were developed to try and calculate the 3D center of rotation for any points located in 3D space. The first algorithm, the vector addition and subtraction, proved to be more cumbersome than it was worth. There were too many potential issues with the algorithm, from the geometry, to knowing exactly which angles were being calculated by MATLAB and to potential bugs in the code, that it made it very difficult to know what was wrong. The symmetry that was exhibited in the movement of the CR was comforting. I feel that that algorithm would be well suited for something that has a large range of motion, but would not be well suited to describe something like the lumbar spine which cannot bend further than 10 degrees.

The 2D projection method that looked at the intersecting point between two normal vectors to the data seems to indicate that it works the best in the exact opposite conditions than the first method. Instead of having a desire for a larger spacing between points, i.e. greater angle of rotation, this method looks to have the points as close

as possible to one another. This could be due to the fact that the data was not interpolated through with a smooth arc that had a smaller step size than the original data. Independent of that idea though, this is good news for any future study that wants to see how the CR moves through space at a higher resolution.

The projects that inspired this work, particularly the lumbar spine analysis, were never finished to completion and therefore this paper has become more of a commentary on the methods that can be used to calculate the 3D center of rotation. There is still room for improving both algorithms and making them more robust and precise, but the finding that the RMSD was $0.27mm$ for the center of rotation of a helix seems to indicate that the current state is not as pessimistic as I had initially thought.

6 Acknowledgements

I would like to thank Dr. Ulrich Schreiber for his initial help on the project during my time at the Technical University of Munich, Dr. David Lomen for his guidance upon my return to the University of Arizona and Dr. David Raichlen for allowing to continue to collect data from his Vicon Motion Capture System.

The DAAD Undergraduate Scholarship also provided the necessary funding for my research and studies in Munich, Germany.

A cr-vector.m

```
function [cr,theta] = cr_vector(X)

%This function will calculate the axis of rotation between two vertebraes
%after having solved for the translational and rotational movement of the
%points. (Biomechanics TUM: Munich, Germany 2007)

%Taking the initial data set and removing a (n x 9) matrix

A = [X(:,1:3),X(:,4:6),X(:,7:9)];
B = [X(:,10:12),X(:,13:15),X(:,16:18)];
n = length(X');

%The angle of rotation of each vertebrae with respect to the plane z = 0

for i = 1:n-1
    p1 = plane(A(i,1:3),A(i,4:6),A(i,7:9));
    p2 = plane(B(i,1:3),B(i,4:6),B(i,7:9));
    G(i) = dot(p1(1,1:3),[0,0,1])/(norm(p1(1,1:3)));
    H(i) = dot(p2(1,1:3),[0,0,1])/(norm(p2(1,1:3)));
    F(i) = dot(p1(1,1:3),p2(1,1:3))/(norm(p1(1,1:3))*norm(p2(1,1:3)));
end
theta_L3 = acos(G(:))*180/pi;
```

```

theta_L4 = acos(H(:))*180/pi;
theta_L3_L4 = acos(F(:))*180/pi;
x1 = 1:1:n-1;

%Here is the calculation to solve for the center of rotation

f = 1;
for i = 1:4:n-2
    r_A = sqrt((A(i,1) - A(i+1,1))^2 + (A(i,2) - A(i+1,2))^2);
    r_B = sqrt((B(i,1) - B(i+1,1))^2 + (B(i,2) - B(i+1,2))^2);
    d_A = sqrt((A(i,1) - A(i+1,1))^2 + (A(i,2) -
        A(i+1,2))^2 + (A(i,3) - A(i+1,3))^2);
    d_B = sqrt((B(i,1) - B(i+1,1))^2 + (B(i,2) -
        B(i+1,2))^2 + (B(i,3) - B(i+1,3))^2);
    zA = A(i+1,3) - A(i,3);
    zB = B(i+1,3) - B(i,3);
    lA = zA/sin(G(i+1) - G(i));
    lB = zB/sin(H(i+1) - H(i));
    betaA = asin(lA/d_A);
    betaB = asin(lB/d_B);
    thetaA = pi - 2*betaA;
    thetaB = pi - 2*betaB;
    cA = (sin(betaA)*d_A)/sin(thetaA);
    cB = (sin(betaB)*d_B)/sin(thetaB);
    xA = sqrt(cA^2 - zA^2);

```

```
xB = sqrt(cB^2 - zB^2);
zetaA = asin(zA/cA);
zetaB = asin(zB/cB);
phiA = acos((r_A^2-xA^2-cA^2)/(2*xA*cA));
phiB = acos((r_B^2-xB^2-cB^2)/(2*xB*cB));
if A(i+1,4) > A(1,4)
    cr_Ax = A(i,4) - cA*cos(phiA/2);
else
    cr_Ax = A(i,4) + cA*cos(phiA/2);
end
if A(i+1,5) > A(1,5)
    cr_Ay = A(i,5) - cA*sin(phiA/2);
else
    cr_Ay = A(i,5) + cA*sin(phiA/2);
end
if A(i+1,6) > A(1,6)
    cr_Az = A(i+1,6) - cA*sin(zetaA);
else
    cr_Az = A(i+1,6) + cA*sin(zetaA);
end
if B(i+1,1) > B(1,1)
    cr_Bx = B(i,1) - cB*cos(phiB/2);
else
    cr_Bx = B(i,1) + cB*cos(phiB/2);
end
```

```
    if B(i+1,2) > B(1,2)
        cr_By = B(i,2) - cB*sin(phiB/2);
    else
        cr_By = B(i,2) + cB*sin(phiB/2);
    end
    if B(i+1,3) > B(1,3)
        cr_Bz = B(i+1,3) - cB*sin(zetaB);
    else
        cr_Bz = B(i+1,3) + cB*sin(zetaB);
    end
    cr_A = [cr_Ax,cr_Ay,cr_Az];
    cr_B = [cr_Bx,cr_By,cr_Bz];
    cr(f,1:6) = [cr_A,cr_B];
    f = f+1;
end
figure
plot3(f,cr_A)
end
```

B plane.m

```
function p = plane (A,B,C)
```

```
%This function takes three points and gives the relevant
%equation of the plane. Note: A, B and C must be rows
```

```
%in a matrix.

double x;
double y;
double z;
n = length(A);
m = length(B);
l = length(C);
if n ~= 3 || m ~= 3 || l ~= 3
    error('The points must be 3D to construct a plane')
end
x = 0;
y = 0;
z = 0;
f = det([x-A(1,1),y-A(1,2),z-A(1,3);x-B(1,1),y-B(1,2),
        z-B(1,3);x-C(1,1),y-C(1,2),z-C(1,3)]);
p(1,4) = f;
x = 1;
y = 0;
z = 0;
p(1,1) = det([x-A(1,1),y-A(1,2),z-A(1,3);x-B(1,1),y-B(1,2),
        z-B(1,3);x-C(1,1),y-C(1,2),z-C(1,3)]) - p(1,4);
x = 0;
y = 1;
z = 0;
```

```

p(1,2) = det([x-A(1,1),y-A(1,2),z-A(1,3);x-B(1,1),y-B(1,2),
             z-B(1,3);x-C(1,1),y-C(1,2),z-C(1,3)]) - p(1,4);
x = 0;
y = 0;
z = 1;
p(1,3) = det([x-A(1,1),y-A(1,2),z-A(1,3);x-B(1,1),y-B(1,2),
             z-B(1,3);x-C(1,1),y-C(1,2),z-C(1,3)]) - p(1,4);

```

C three-d.m

```

function cr = three_d(x,y,z,k)

%The main program that solves for the 3D center of rotation.

n = length(x);
j=1;
clear cr
for i = 1:k:n-k
    grad_x = abs(sum(gradient(x(i:i+k)))));
    grad_y = abs(sum(gradient(y(i:i+k)))));
    grad_z = abs(sum(gradient(z(i:i+k)))));
    min_grad = min([grad_x grad_y grad_z]);
    if min_grad == grad_x
        x_new = z(i:i+k);

```

```

y_new = y(i:i+k);
z_new = x(i:i+k);
to = 1;
elseif min_grad == grad_y
y_new = z(i:i+k);
x_new = x(i:i+k);
z_new = y(i:i+k);
to = 2;
else
x_new = x(i:i+k);
y_new = y(i:i+k);
z_new = z(i:i+k);
to = 3;
end
init_point = two_d(x_new,y_new);
XI = plane([x_new(1+k/5) y_new(1+k/5) z_new(1+k/5)],
            [x_new(1+2*k/5) y_new(1+2*k/5) z_new(1+2*k/5)],
            [x_new(1+4*k/5) y_new(1+4*k/5) z_new(1+4*k/5)]);
if to == 3
z_coord = (-XI(1,4) - XI(1,1)*init_point(1,1) -
            XI(1,2)*init_point(2,1))/XI(1,3);
cr(j,1:3) = [init_point(1,1) init_point(2,1) z_coord];
elseif to == 1
x_coord = (-XI(1,4) - XI(1,3)*init_point(1,1) -
            XI(1,2)*init_point(2,1))/XI(1,1);

```

```

        cr(j,1:3) = [x_coord init_point(2,1) init_point(1,1)];
    else
        y_coord = (-XI(1,4) - XI(1,1)*init_point(1,1) -
                    XI(1,3)*init_point(2,1))/XI(1,2);
        cr(j,1:3) = [init_point(1,1) y_coord init_point(2,1)];
    end
    hold on
    plot3(cr(j,1),cr(j,2),cr(j,3),'ko')
    j = j+1;
end
plot3(x,y,z,'ro')
hold off
end

```

D two-d.m

```
function cr = two_d(x,y)
```

```
%Finds the intersection point of two normal vectors from the given data.
```

```
%This point defines the center of rotation.
```

```
dx = gradient(x);
```

```
dy = gradient(y);
```

```
N = [-dy dx];
```

```

m1 = N(round(2/5*length(x)),2)/N(round(4/5*length(x)),1);
c1 = y(round(2/5*length(x))) - m1*x(round(4/5*length(x)));
m2 = N(round(4*length(x)/5),2)/N(round(4*length(x)/5),1);
c2 = y(round(4*length(x)/5)) - m2*x(round(4*length(x)/5));
A = [-m1 1;-m2 1];
b = [c1;c2];
cr = A\b;
end

```

E World Congress 2009- Medical Physics and Biomedical Engineering Conference Abstract

Modeling the 3-Dimensional Center of Rotation of a Total Disc Arthroplasty at L4/5

I. Grubisic^{1,3}, U. Schreiber² and C. Birkenmaier¹

1 Department of Orthopaedics, Grosshadern Medical Center, University of Munich, Munich, Germany 2 Department of Cardiovascular Surgery, German Heart Center Munich, Technische Universitt Mnchen, Germany 3 Mathematics Department, University of Arizona, Tucson, Arizona

Abstract- In recent years, total disc arthroplasty (TDA) has increasingly been competing with fusion surgery for the surgical treatment of painful degenerative disc disease (DDD) of the lumbar spine. It is generally accepted notion, that increased mechanical stress on the motion segment adjacent to a fusion is a key reason for the development of adjacent segment degeneration. There is discussion, however, whether the biomechanical properties of

the types of TDA currently available are similar enough to those of a native motion segment in order to avoid undesired side-effects, such as overloading and premature degeneration of the facet joints. Since some of the current models of TDA possess constrained kinematics, the 3-dimensional center of rotation (CR) is of particular interest in such considerations. The biomechanical and mathematical study presented here is designed to investigate whether a valid mathematical model of the 3-dimensional center of rotation can be derived from biomechanical data.

Keywords- biomechanics; spine; motion preservation, adjacent segment degeneration, total disc replacement, total disc arthroplasty

I. INTRODUCTION

Until some years ago, despite limited data as to the mid-and long-term clinical outcomes, fusion surgery was the standard therapy for painful lumbar degenerative disc disease (DDD). Between 1996 and 2001, these procedures were being performed with an annual growth rate of 113 percent (USA) and have reached a level of 200,000 operations per year 1. Adjacent level degeneration as a result of increased mechanical stress on the motion segment next to the fused segment is thought to be the single major biomechanical disadvantage of lumbar fusion surgery 2-5. While there are experimental indications that the free motion segment adjacent to a fused level indeed is subject to increased mechanical stress 6-10, other data suggest that this may not be the case or to some extent is dependent on the surgical technique 11 and the (correct) reconstruction of the sagittal profile 12. Total disc arthroplasty (TDA) is designed to surgically treat DDD while preserving motion, thus avoiding adjacent segment degeneration. The data from the US-American FDA trials with the Prodisc L and the Charit III indicate that

these implants are not inferior to fusion during the trial period and that they may have some advantage over fusion with regards to postoperative rehabilitation 13, 14. As of yet, there are no long-term results from randomized controlled trials available for TDA, but there are first publications of undesired side-effects and failures from facet joint overload, accelerated facet joint degeneration and premature implant wear 15-18. This raises the question about the 3-dimensional center of rotation (CR) of such implants as compared to the native motion segment, since it is a major determinant of biomechanical comparability and compatibility. This study investigates the development of a mathematical algorithm for the use of biomechanical motion data for the modeling of the 3-dimensional center of rotation for TDA.

II. MATERIAL AND METHODS

Preparation of Spine and VICON

A pedicle screw with 3 reflective markers will be inserted into vertebrae L4 to L1. This will be done for both the native and operated spine. An x-ray image of the operated spine is shown in Figure 1. Six infrared VICON cameras will then be used to collect the three dimensional coordinates of the reflective markers.

MATLAB Description and Assumptions

It has been hypothesized that the CR is not a fixed point within the lumbar spine. This stipulation requires that an iterative method be used. The iterative method is not necessarily a numerical solution though. It means that the data points are broken down into subgroups and the CR is solved for from each subgroup. The CR for each subgroup will be solved in the 2D space by a projecting down the axis that exhibited the least movement. Additional steps involve interpolating the projected curve using a spline function in MATLAB and then refining the curve by interpolating with $x =$

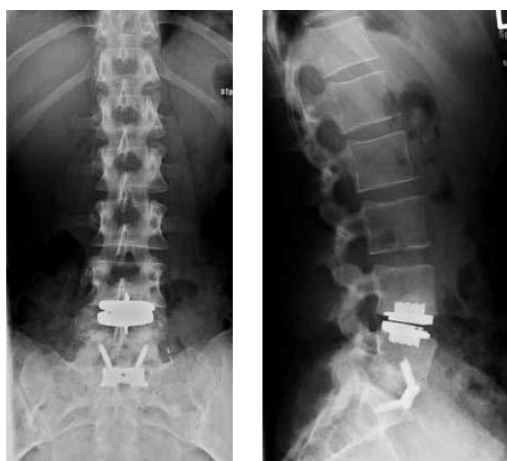


Figure 5: Fig. 1 Patient after hybrid treatment with stand-alone ALIF (Synfix) at L5/S1 and TDR (Prodisc) at L4/5 through a single anterior approach

$\cos(t)$ and $y = \sin(t)$. The CR will then be the intersection point of the normal vectors to this smooth curve.

The primary and most important assumption is that no translational motion occurs during any of the subgroups. This is appropriate because the VICON cameras can collect data up to 200Hz, along with a slow bending of the spine at 50mm/s, makes it possible to decompose subgroups without translational motion. A subsequent assumption which follows is that the data points of a subgroup can all be explained by a single plane. This is important when solving for the third coordinate of the CR.

III. RESULTS

Figure 2(a) shows a very simplified case where the rotation and translation of the points are moving along the z-axis. The data was simulated by manually creating a helix in MATLAB. After applying the above mentioned algorithm, with the exception of a few outliers, the results were very consistent. Taking the outliers into account, a RMSD value of 2.1 is reported. It is appropriate to get rid of the outliers because it is reasonable to assume that the movement of the CR through space should be a smooth curve if the data is also a smooth curve. When removing the outliers in Figure 2(b), the RMSD decreases to 0.2 which is less than what is expected for the translation of the CR. The units were dimensionless in this case, but it could be compared to the millimeter scale that is used by VICON. This means that the algorithm should be able to within statistical error determine whether or not the CR is moving in the lumbar spine.

The same as Figure 3(b) from main paper

Fig. 2 Using MATLAB to solve for the center of rotation of a helix. (a) The plot with all of the calculated values. The actual center of rotation is marked by a 'o' where

the calculated is a 'x'. (b) The plot with the three main outliers excluded. The same symbols were used as in part (a).

IV. DISCUSSION

Applying the algorithm to existing VICON data is more problematic though. Even though there has been success at the level of ideal data, it has been limited when using real 3D captured data. The noise in the system, and also the high frequency of data collection pose problems for MATLAB because the data points are often times too close to one another. Close proximity of data points leads to problems because the algorithm is looking for an intersection point between two nearly parallel lines. This causes the problem to become poorly conditioned and difficult to solve analytically. A numerical solution should be attempted as well.

V. CONCLUSIONS

By comparing how the center of rotation differs between the native and operated spines, it will allow us to analyze the change in shearing and torque forces that are being exerted on the lumbar column. This allows for a long-term estimation of the effect on the adjacent segments of the implant.

ACKNOWLEDGMENT

DAAD Undergraduate Study Abroad Scholarship.

REFERENCES 1. Deyo RA, Gray DT, Kreuter W, Mirza S, Martin BI. United States trends in lumbar fusion surgery for degenerative conditions. *Spine* 2005;30(12):1441-5; discussion 6-7. 2. Miyamoto K. [Long-term follow-up results of anterior discectomy and interbody fusion for lumbar disc herniation]. *Nippon Seikeigeka Gakkai Zasshi* 1991;65(12):1179-90. 3. Kumar MN, Jacquot F, Hall H. Long-term follow-up of func-

tional outcomes and radiographic changes at adjacent levels following lumbar spine fusion for degenerative disc disease. *Eur Spine J* 2001;10(4):309-13. 4. Hilibrand AS, Robbins M. Adjacent segment degeneration and adjacent segment disease: the consequences of spinal fusion? *Spine J* 2004;4(6 Suppl):190S-4S. 5. Park P, Garton HJ, Gala VC, Hoff JT, McGillicuddy JE. Adjacent segment disease after lumbar or lumbosacral fusion: review of the literature. *Spine* 2004;29(17):1938-44. 6. Rao RD, David KS, Wang M. Biomechanical changes at adjacent segments following anterior lumbar interbody fusion using tapered cages. *Spine* 2005;30(24):2772-6. 7. Chiang MF, Zhong ZC, Chen CS, Cheng CK, Shih SL. Biomechanical comparison of instrumented posterior lumbar interbody fusion with one or two cages by finite element analysis. *Spine* 2006;31(19):E682-9. 8. Chen CS, Feng CK, Cheng CK, Tzeng MJ, Liu CL, Chen WJ. Biomechanical analysis of the disc adjacent to posterolateral fusion with laminectomy in lumbar spine. *J Spinal Disord Tech* 2005;18(1):58-65. 9. Chosa E, Goto K, Totoribe K, Tajima N. Analysis of the effect of lumbar spine fusion on the superior adjacent intervertebral disk in the presence of disk degeneration, using the three-dimensional finite element method. *J Spinal Disord Tech* 2004;17(2):134-9. 10. Goto K, Tajima N, Chosa E, et al. Effects of lumbar spinal fusion on the other lumbar intervertebral levels (three-dimensional finite element analysis). *J Orthop Sci* 2003;8(4):577-84. 11. Lai PL, Chen LH, Niu CC, Fu TS, Chen WJ. Relation between laminectomy and development of adjacent segment instability after lumbar fusion with pedicle fixation. *Spine* 2004;29(22):2527-32; discussion 32. 12. Akamaru T, Kawahara N, Tim Yoon S, et al. Adjacent segment motion after a simulated lumbar fusion in different sagittal alignments: a biomechanical analysis. *Spine* 2003;28(14):1560-6. 13. Delamarter RB, Bae HW, Pradhan BB. Clinical results of ProDisc-II lumbar total disc replacement: report from the United States clinical trial. *Orthop Clin North Am* 2005;36(3):301-13. 14.

McAfee PC, Cunningham B, Holsapple G, et al. A prospective, randomized, multicenter Food and Drug Administration investigational device exemption study of lumbar total disc replacement with the CHARITE artificial disc versus lumbar fusion: part II: evaluation of radiographic outcomes and correlation of surgical technique accuracy with clinical outcomes. *Spine* 2005;30(14):1576-83; discussion E388-90. 15. Stieber JR, Donald GD, 3rd. Early failure of lumbar disc replacement: case report and review of the literature. *J Spinal Disord Tech* 2006;19(1):55-60. 16. Bertagnoli R, Zigler J, Karg A, Voigt S. Complications and strategies for revision surgery in total disc replacement. *Orthop Clin North Am* 2005;36(3):389-95. 17. Kostuik JP. Complications and surgical revision for failed disc arthroplasty. *Spine J* 2004;4(6 Suppl):289S-91S. 18. van Ooij A, Oner FC, Verbout AJ. Complications of artificial disc replacement: a report of 27 patients with the SB Charite disc. *J Spinal Disord Tech* 2003;16(4):369-83.

Author: Ivan Grubisic Institute: Department of Orthopaedics, Grosshadern Medical Center Street: Marchioninistrasse 15 City: Munich Country: Germany Email: ivan.grub@googlemail.com